Journal of Aerosol Science 46 (2012) 64–76

Contents lists available at SciVerse ScienceDirect

Journal of Aerosol Science

journal homepage: www.elsevier.com/locate/jaerosci

A procedure to assess local and long-range transport contributions to $PM_{2.5}$ and secondary inorganic aerosol

Stefania Squizzato, Mauro Masiol, Elena Innocente, Eliana Pecorari, Giancarlo Rampazzo, Bruno Pavoni *

Dipartimento di Scienze Ambientali, Informatica e Statistica, Università Ca' Foscari Venezia, Calle Larga Santa Marta 2137, Dorsoduro, Venice 30123, Italy

ARTICLE INFO

Article history:
Received 5 May 2011
Received in revised form
30 November 2011
Accepted 5 December 2011
Available online 17 December 2011

Keywords:
$PM_{2.5}$
Ionic composition
Secondary inorganic aerosol
Local contribution
Long-range transport

ABSTRACT

All over Europe, low wind speeds and stable atmospheric stratification are meteorological factors leading to air pollution episodes. Discriminating the contribution of the local atmospheric circulation and the regional and long-range transport processes, in determining $PM_{2.5}$ and pollutants levels, is very important for deciding any effective abatement measure. This is particularly true in the Northeastern part of the Po Valley, one of the most polluted areas in Europe.

This study proposes a method for assessing the relative importance of regional and long-range transport episodes and of local sources on $PM_{2.5}$ mass and ionic composition.

Air mass back-trajectories were combined with PM chemical composition and local wind data and the relative contributions were estimated.

Air mass histories show that the levels of $PM_{2.5}$ increased when air masses had arrived from Northern to Central and Northwestern Europe and significantly dropped when the trajectories originated from the Mediterranean area. Furthermore, results reveal that relatively fast winds from quadrant I were associated with clean air and increasing sea-salt components. Diversely, air mass stagnations were closely accompanied by severe pollution events. Heavily polluted episodes were recorded in correspondence of days characterized by low-mobility atmospheric conditions and when air masses had spent most time over the Po Valley region.

These results can help understanding the sources, the chemistry and dynamics of $PM_{2.5}$ in Northeastern Italy. The proposed approach is easily applicable to other environments.

1. Introduction

The recent Council Directive 2008/50/EC (EC, 2008) has attributed great importance to the monitoring of fine particulate matter (with an aerodynamic diameter <2.5 μm, $PM_{2.5}$) in Europe. The main problem associated with $PM_{2.5}$ is the strong correlation between its air concentration and some adverse health effects, ranging from inflammatory potential and pulmonary diseases to cardiovascular troubles and mortality (Pope & Dockery, 2006; Polichetti et al., 2009). Most studies concluded that particulate matter is the main pollutant causing deaths in Europe today (EEA, 2005).

The resulting new annual limit value for $PM_{2.5}$ is fixed to 25 μg m^{-3} to be met in 2015 and it will become progressively more restrictive in 2020. This goal is not, or not yet achieved in several European sites so far (EEA, 2010). In particular,

* Corresponding author. Tel.: +390412348522; fax: +390412348582.
E-mail address: brown@unive.it (B. Pavoni).

0021-8502/$ - see front matter © 2011 Elsevier Ltd. All rights reserved.
doi:10.1016/j.jaerosci.2011.12.001

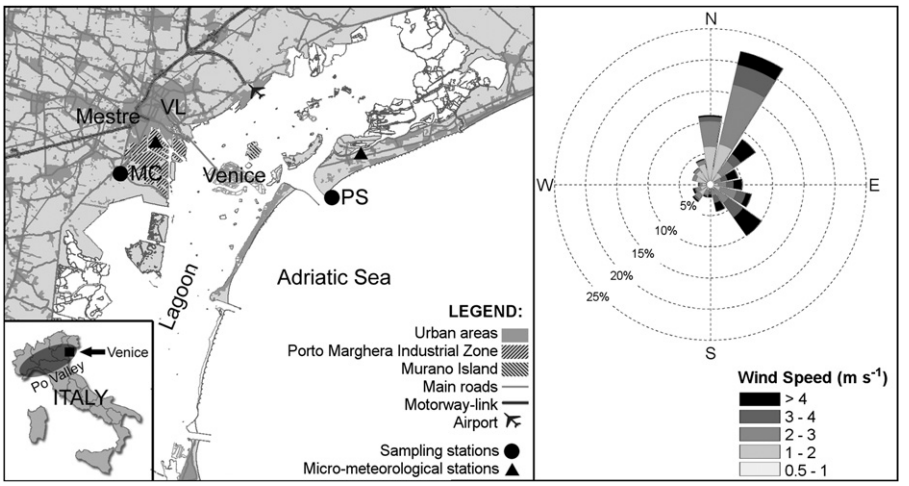

Fig. 1. Study area and wind rose relative to 2009.

some studies (Hazenkamp-von Arx et al., 2004; Putaud et al., 2004; Putaud et al., 2010) indicated that particulate matter pollution increases from North to central and Southern Europe. The most worrying situations are reported during the cold season in medium and large cities and, in general, in Benelux and Northern Italy, where high air pollution may cause serious risks for human health (EC, 2004).

All over Europe, low wind speeds and stable atmospheric stratification seem to be key meteorological factors leading to air pollution episodes. In Southern and Central Europe stable atmospheric stratification, low wind speeds, mesoscale circulation patterns, topography and solar radiation are the most important factors (Valkama & Kukkonen, 2004). Furthermore there is evidence that transport of particulate matter over large distances following prevailing winds may affect air quality in urban and rural areas of Southern Europe (i.e., Salvador et al., 2008; Glavas et al., 2008). For this reason, knowing the relationship between the local atmospheric circulation and the regional and long-range transport processes, in contributing to $PM_{2.5}$ and pollutants levels, has become very important for deciding any effective abatement measure

In the Po Valley (Fig. 1), which extends for a great part of Northern Italy and is recognized as the most industrialized and populated region of Italy, with large cities such as Turin, Milan, Verona, Boulogne and Venice-Mestre, air quality is strongly affected by anthropogenic emissions. However, there is evidence that problems with air pollution are principally due to unfavorable weather conditions and orographic features, which reduce air mass circulation and favor pollutant accumulation.

In Europe, $PM_{2.5}$ is mainly composed of carbonaceous materials and salts of sulfate, nitrate and ammonium, which are the main constituents of the secondary inorganic aerosol (SIA) (Putaud et al., 2010). The concentrations and formation mechanisms of $PM_{2.5}$ and SIA were already studied in some sites of Po Valley such as San Pietro Capofiume (Boulogne), Milan, Venice Lagoon (see e.g., Hamed et al., 2007; Sogacheva et al., 2007; Lonati et al., 2008; Prodi et al., 2009), but relatively scarce data are available for the Eastern part of the Po plain. In particular only few studies reported on air quality in the Venice-Mestre area (Rampazzo et al., 2008a, 2008b; Stortini et al., 2009; Masiol et al., 2010) and mainly discussed element characterization, source identification and apportionment.

The present paper proposes a method for discriminating the contribution of local emission processes, regional and long-range scale transport mechanisms to $PM_{2.5}$, ionic fraction and SIA, in urban, industrial and semi-rural coastal background sites. The main goal is to highlight the specific local atmospheric circulation pattern and to identify regional and long-range transport pathways that may have an impact on pollutant levels. The proposed approach includes 4 main steps: (i) a cluster analysis is computed on daily back trajectories and the average ion concentration is defined for each cluster to determine the importance of long-range transport processes; (ii) experimental chemical data are interpreted in terms of local atmospheric circulation: samples are grouped by a *q*-mode hierarchical cluster analysis (*q*HCA) and all groups are subsequently interpreted according to wind speed and direction; (iii) groups resulting by *q*HCA are related to clusters from back-trajectories to assess the relative importance of local circulation, regional and long-range transport processes on air quality and then (iv) local contribution was estimated using the Lenschow approach (Lenschow et al., 2001).

2. Study area

The Venice-Mestre area is located between the Po Valley and the Adriatic Sea (Fig. 1). The emissive scenario is common to other continental districts of Po Valley and includes: (i) an extended urban area, Mestre, with about 270,000 inhabitants; (ii) an extended industrial zone, Porto Marghera ($\sim$12 km^2), with chemical and metallurgical works, oil-refineries, incineration and thermoelectric power plants burning coal, gas and refuse derived fuel; (iii) several heavy traffic city roads, a highway and a causeway. The peculiarity of this area is the city center of Venice in the middle of

a ~550 km^2-wide lagoon, almost free from automotive traffic, but affected by: (i) artistic glass factories emissions in the island of Murano; (ii) exhausts from public, commercial and tourist shipping and (iii) sea-spray from the Adriatic Sea and the Lagoon (Rampazzo et al., 2008a, 2008b; Stortini et al., 2009; Rossini et al., 2010; Masiol et al., 2010).

Fig. 1 shows the wind roses plots calculated for 2009 in the study area. Annually, the predominant wind direction is NNE, with an average wind speed of 2.5 m s^{-1} and ~4% wind calm (< 0.5 m s^{-1}). Winds from W and NE increase during autumn and winter, due to the occurrence of a nocturnal breeze, northeast and northwest winds. Direction from SE is however predominant during the warm season for an increase of sea/land breeze circulation.

3. Materials and methods

3.1. Sampling

$PM_{2.5}$ samples were collected in the framework of a project aiming at characterizing the atmospheric aerosol in the Venice area by means of chemical analyses and modeling approaches (Centanni et al., 2009). The sampling campaign has been extended for one year in three sites selected to be representative of different emissive scenarios (Fig. 1):

- The station **Via Lissa** (VL; Lat. N 45.4871–Long. E 12.2229) is located near the buildings of the Environmental Protection Agency of Veneto Region (ARPAV) in a highly populated residential zone of Mestre surrounded by several heavy traffic roads (distance > 50 m). The site was categorized as *urban background* (ARPAV, 2010a). Moreover, VL lies about 200 m far from an important motorway and few meters from the railway;
- **Malcontenta** (MC; Lat. N 45.4382–Long. E 12.2055) is a station of the ARPAV regional monitoring network, categorized as *industrial* (ARPAV, 2010b). It is located in the surroundings of the industrial zone of Porto Marghera and it was selected on the basis of previous modeling simulations (Centanni et al., 2009), as a site of industrial fall-out;
- **Punta Sabbioni** (PS; Lat. N 45.4227–Long. E 12.4368) is located mid-height on the lighthouse of Punta Sabbioni on the Adriatic coastline. According to EC classification (2008), this site is a *semi-rural-coastal background*, for being not directly influenced by agglomerations or industrial sites, and located upwind to main emission sources (Fig. 1).

About 150 samples were collected simultaneously in each site (total of 449) on 47 mm quartz fiber filters (Whatman QMA) using low volume automatic samplers equipped with $PM_{2.5}$ cut-off inlets and set according to EN 14907 standard (CEN, 2005). Since strong qualitative and quantitative seasonal variations in chemical composition of particulate matter were commonly reported in the study area, the adopted strategy was to focus the chemical analyses on four sampling periods selected for being representative of different seasons. In particular, the sampling was carried out in spring (37 day, from March to April 2009), summer (36 day from June to July 2009), autumn (42 day from September to October 2009) and winter (41 day from December 2009 to January 2010). Sampling time was 24-h, from 0:00 to 24:00 local time.

3.2. Analytical procedures

$PM_{2.5}$ masses were measured by gravimetric determination (microbalance with 1 μg sensitivity) on filters preconditioned for ~48 h at constant temperature (20 ± 5 °C) and relative humidity (50 ± 5%). Half of each sample was extracted for 1 h in 15 mL ultrapure water (resistivity ≈ 18 MΩ cm) in an ultrasonic bath, whose water temperature was kept < 35 °C to avoid artifacts and evaporation. Filtrates were stored at 4 °C in clean bottles until analyses. After filtration through microporous PTFE membranes (PALL Acrodisc CR, pore size 0.45 μm), four anions (F^-, Cl^-, NO_3^-, SO_4^{2-}) and five cations (Na^+, NH_4^+, K^+, Mg^{2+}, Ca^{2+}) were determined by ion chromatography (IC, Dionex DX500 system), using a guard column (Dionex Ionpac AG14 for anions and CG12 for cations), a separation column (Dionex Ionpac AS14 for anions and CS12 for cations), a self-regenerating suppressed conductivity detector (Dionex ED40) and a gradient pump (Dionex GP40). An isocratic flow of 1.2 L min^{-1} and a 3.5 mM-Na_2CO_3/1.0 nM $NaHCO_3$ (pH 7.5) base eluent were used for anion detection, whereas an isocratic flow 1 L min^{-1} and 20 mN ultrapure H_2SO_4 (pH 1.8) acid eluent for cation analyses.

3.3. Quality control and assurance

Filter blanks and field blanks (kept inside the sampler, but not used for air filtering) were prepared and analyzed together with the samples, following the same procedures; obtained values were routinely subtracted. Means (in μg) and standard deviations of all blanks are: 4 ± 3 F^-, 2 ± 1 Cl^-, 1.6 ± 0.6 NO_3^-, 1.4 ± 0.3 SO_4^{2-}, 28 ± 22 Na^+, 2 ± 1 NH_4^+, 0.9 ± 0.6 K^+, 4 ± 4 Mg^{2+}, 26 ± 19 Ca^{2+}.

Single- and multi-ionic standards for IC (Fluka–Riedel de-Haën) were used to test the linearity and calibrate the instrumental responses. The limit of detections (LODs) were calculated for each ion in each period as three times the standard deviation of the blank values (ng m^{-3}, considering the average air volume sampled): F^- (3.3), Cl^- (3), NO_3^- (2.4), SO_4^{2-} (2.6), Na^+ (6.3), NH_4^+ (3.6), K^+ (4.8), Mg^{2+} (6.8), Ca^{2+} (14.5).

Accuracy of analytical procedures was routinely confirmed by analyzing NIST SRM 1648 standard for air particulate. The recoveries of each ion were in the range of 90–100%. The relative standard deviation of each ion determination was < 5%.

3.4. Micro-meteorology and air mass back-trajectories

Wind speed and direction were hourly measured at two weather stations (Fig. 1) and were used as follows: (i) data from station 5 of Ente della Zona Industriale di Porto Marghera, for VL and MC sites; (ii) from Cavallino-Tre Porti station of ARPAV-Centro Meteorologico di Teolo for PS site.

Back-trajectories, computed from archived meteorological data, are useful to identify the regions where pollutants measured at a site have originated. In this study, 96-hours air mass back-trajectories were simulated using NOAA/ARL hybrid single-particle Lagrangian integrated trajectory (HYSPLIT 4) model (Rolph, 2011; Draxler & Rolph, 2011) and global data assimilation system (GDAS1) meteorological data fields. A starting height within the mixing layer (H_{mix}) conditions was used. H_{mix} is the mixing-layer height calculated using the specific meteorological models MINERVE (Aria Technologies, 2001) and SURFPRO (Arianet, 2005).

As accuracy in back trajectory calculation is decreasing with distance and time (due to model assumptions and spatial and temporal resolution of the meteorological data), 4-day trajectories were considered the most suitable option. Moreover, clustering back-trajectories reduces errors associated to single trajectories (Stohl, 1998).

3.5. Data treatment

The concentrations of $PM_{2.5}$, WSIIs and SIA were inter-correlated and interpreted to evaluate seasonal and spatial variation by one-way ANOVA and correlation coefficients.

With the aim of estimating the influence of regional and long-range transport processes in the area, experimental data have been examined on the bases of air mass origin. A cluster analysis on daily back-trajectories was qualitatively used to classify trajectories into groups of similar history, i.e. similar advection path and velocity. The cluster analysis was applied using HYSPLIT (Draxler et al., 2009). Then, for each cluster average $PM_{2.5}$ concentration and composition were calculated.

Afterwards, to select groups of samples on the basis of their similar ionic composition, a *q*-mode Hierarchical Cluster Analysis (*q*HCA, using Ward's agglomerative method and the squared Euclidean distance measures) was performed on a standardized (mean=0; standard deviation=1) dataset, including Cl^-, NO_3^-, SO_4^{2-}, Na^+, NH_4^+ and K^+. The results have been interpreted on the basis of the local atmospheric circulation to highlight specific wind regimes affecting PM and WSIIs levels. The *q*HCA was repeated for each site, some groups were selected and the average $PM_{2.5}$ and WSII concentrations for each group were calculated. Finally wind roses were plotted and interpreted for the days of each group.

Finally, to assess the relative importance of local circulation, regional and long-range transport processes on air quality, air mass back trajectories were related to each cluster individuated by *q*HCA and local contributions were estimated using the Lenschow approach, considering PS site as representative of regional background levels and including only VL and MC samples characterized by higher concentrations than in PS.

4. Results and discussion

4.1. $PM_{2.5}$ concentration and ionic composition

Table 1 summarizes the average seasonal and annual values for each site. The $PM_{2.5}$ annual mean was 33 $\mu g\,m^{-3}$ for the two mainland sites (VL, MC) and 26 $\mu g\,m^{-3}$ for PS. Compared to the target values proposed by 2008/50/CE, to be attained in 2010, the average values for VL and MC exceed the yearly average of 25 $\mu g\,m^{-3}$, even beyond the margin of tolerance (+20%).

Large variations in $PM_{2.5}$ mass concentrations were observed in the area. Generally the concentrations of the $PM_{2.5}$ were inversely correlated with the air temperature, with higher levels during the cold period. Comparing these results with historical data (ARPAV, 2010a, 2010b), available since 2008 for VL and MC, seasonal means appear to have dropped from January to October, and contrarily increased in November and December.

Along with the results for each ion, Table 1 also reports statistics for non-sea-salt sulfate ($nssSO_4^{2-}$), indirectly calculated using the seawater ratio, $nssSO_4^{2-} = SO_4^{2-} - 0.25 * Na^+$. WSIIs account for a large part of $PM_{2.5}$ mass, ranging from 4% to 70% (mean 34%). On annual basis, NO_3^-, SO_4^{2-} and NH_4^+ were the most abundant ions in all sites, contributing ~90% of the total ion concentration. At VL site nitrate accounts for 12% of $PM_{2.5}$ mass, followed by sulfate (10%) and ammonium (7%), whereas the contributions of Na^+, K^+, Ca^{2+} and Cl^- are very limited (1%). Results for MC are quite similar: nitrate and sulfate (11%), ammonium (7%). In PS nitrate accounts for 15%, sulfate (13%), ammonium (8%); Na^+, K^+ and Cl^- never exceed 1%.

4.2. Secondary inorganic aerosol estimation

SIA is produced in the atmosphere through (photo-) chemical reactions of some gaseous precursors such as NO_x, SO_2, NH_3, which may react with O_3 and other reactive molecules (including radicals) to mainly form ammonium nitrate (NH_4NO_3) and ammonium sulfate ($(NH_4)_2SO_4$). The SIA formation strongly depends on the atmospheric conditions and availability of its precursor gasses: Ammonia first neutralizes sulfuric acid to ammonium bisulfate $(NH_4)HSO_4$ and ammonium sulfate $(NH_4)_2SO_4$. The remaining NH_3 may also react with nitric acid to ammonium nitrate (NH_4NO_3).

Table 1
Seasonally and annually statistics (median, mean) of experimental values.

	Spring			Summer			Autumn			Winter			Annual		
	N	Median	Mean	N	Median	Mean	N	Median	Mean	N	Median	Mean	N	Median	Mean
Via Lissa (VL)—Urban background															
$PM_{2.5}$ ($\mu g\,m^{-3}$)	37	28	37	36	15	15	38	28	30	38	50	51	149	27	33
F^- ($\mu g\,m^{-3}$)	30	0.03	0.06	12	0.05	0.04	11	0.01	0.01	13	0.06	0.07	66	0.03	0.05
Cl^- ($\mu g\,m^{-3}$)	36	0.08	0.17	24	0.01	0.02	34	0.06	0.10	38	0.46	0.52	132	0.09	0.23
NO_3^- ($\mu g\,m^{-3}$)	37	3.4	6.4	36	0.4	0.5	38	0.9	2.9	38	4.7	6.1	149	1.7	4.0
SO_4^{2-} ($\mu g\,m^{-3}$)	37	1.8	2.4	36	2.6	2.7	38	3.8	4.3	38	3.2	3.8	149	2.5	3.3
$nssSO_4^{2-}$ ($\mu g\,m^{-3}$)	37	1.7	2.3	36	2.6	2.6	38	3.7	4.3	38	3.2	3.8	149	2.5	3.2
Na^+ ($\mu g\,m^{-3}$)	36	0.1	0.3	35	0.1	0.3	38	0.1	0.1	36	0.1	0.1	145	0.1	0.2
NH_4^+ ($\mu g\,m^{-3}$)	37	1.4	2.4	35	1.0	1.0	38	1.9	2.4	38	3.5	3.3	148	1.6	2.3
K^+ ($\mu g\,m^{-3}$)	37	0.2	0.3	35	0.1	0.1	38	0.2	0.2	38	0.5	0.6	148	0.2	0.3
Mg^{2+} ($\mu g\,m^{-3}$)	31	0.04	0.05	26	0.02	0.04	28	0.02	0.03	29	0.02	0.04	114	0.02	0.04
Ca^{2+} ($\mu g\,m^{-3}$)	32	0.3	0.4	25	0.2	0.3	26	0.1	0.1	6	0.1	0.1	89	0.2	0.3
SIA ($\mu g\,m^{-3}$)	37	6.6	11.1	36	3.9	4.0	38	7.7	9.6	38	13.0	13.1	149	6.5	9.5
SIA (%)	37	26	26	36	27	26	38	28	28	38	26	26	149	26	27
$\sum$WSII ($\mu g\,m^{-3}$)	37	7.3	12.3	36	4.4	4.7	38	8.4	10.2	38	14.3	14.5	149	7.4	10.5
$\sum$WSII (%)	37	32	32	36	32	32	38	30	31	38	29	28	149	31	30
Malcontenta (MC)—Industrial															
$PM_{2.5}$ ($\mu g\,m^{-3}$)	30	30	32	33	15	18	42	30	30	41	50	50	146	29	33
F^- ($\mu g\,m^{-3}$)	30	0.08	0.15	20	0.03	0.04	28	0.04	0.05	20	0.05	0.07	98	0.04	0.08
Cl^- ($\mu g\,m^{-3}$)	30	0.26	0.49	31	0.01	0.05	42	0.08	0.11	41	0.48	0.52	144	0.13	0.29
NO_3^- ($\mu g\,m^{-3}$)	30	5.3	5.4	33	0.3	0.7	42	1.1	2.9	41	4.7	5.8	146	2.5	3.7
SO_4^{2-} ($\mu g\,m^{-3}$)	30	2.3	2.4	33	2.2	3.4	42	3.7	4.4	41	3.6	3.9	146	2.7	3.6
$nssSO_4^{2-}$ ($\mu g\,m^{-3}$)	30	2.2	2.3	33	2.2	3.3	42	3.6	4.4	41	3.6	3.9	146	2.6	3.6
Na^+ ($\mu g\,m^{-3}$)	29	0.3	0.5	33	0.2	0.3	42	0.1	0.1	41	0.1	0.1	145	0.1	0.2
NH_4^+ ($\mu g\,m^{-3}$)	30	2.3	2.3	33	0.9	0.9	42	1.8	2.4	41	3.5	3.4	146	1.8	2.3
K^+ ($\mu g\,m^{-3}$)	30	0.2	0.3	33	0.1	0.1	42	0.2	0.2	41	0.5	0.6	146	0.2	0.3
Mg^{2+} ($\mu g\,m^{-3}$)	30	0.05	0.06	32	0.03	0.05	28	0.02	0.03	23	0.03	0.04	113	0.03	0.05
Ca^{2+} ($\mu g\,m^{-3}$)	30	0.4	0.4	19	0.2	0.7	27	0.2	0.3	18	0.2	0.3	94	0.2	0.4
SIA ($\mu g\,m^{-3}$)	30	9.7	10.0	33	4.0	4.9	42	7.4	9.6	41	13.3	13.1	146	7.7	9.6
SIA (%)	30	32	32	33	26	26	42	29	29	41	26	27	146	28	28
$\sum$WSII ($\mu g\,m^{-3}$)	30	11.6	12.0	33	4.2	5.9	42	8.0	10.3	41	14.2	14.5	146	9.0	10.8
$\sum$WSII (%)	30	40	40	33	30	31	42	33	31	41	29	30	146	32	32
Punta Sabbioni (PS)—Rural-coastal background															
$PM_{2.5}$ ($\mu g\,m^{-3}$)	37	21	27	36	11	11	40	24	26	41	38	38	154	21	26
F^- ($\mu g\,m^{-3}$)	13	0.01	0.04	1	0.01	0.01	0	–	–	11	0.03	0.03	25	0.02	0.04
Cl^- ($\mu g\,m^{-3}$)	37	0.27	0.33	36	0.03	0.04	40	0.11	0.16	41	0.37	0.44	154	0.17	0.25
NO_3^- ($\mu g\,m^{-3}$)	37	4.2	5.8	36	0.5	0.9	40	1.3	3.5	41	4.0	5.1	154	2.3	3.9
SO_4^{2-} ($\mu g\,m^{-3}$)	37	2.2	2.4	36	2.4	2.7	40	3.3	4.6	41	3.4	4.0	154	2.5	3.5
$nssSO_4^{2-}$ ($\mu g\,m^{-3}$)	37	2.1	2.3	36	2.4	2.7	40	3.2	4.5	41	3.3	4.0	154	2.4	3.4
Na^+ ($\mu g\,m^{-3}$)	37	0.2	0.2	34	0.1	0.1	40	0.3	0.4	38	0.1	0.2	149	0.2	0.2
NH_4^+ ($\mu g\,m^{-3}$)	37	1.7	2.2	36	1.0	1.1	40	2.1	2.6	40	2.7	2.9	153	1.7	2.2
K^+ ($\mu g\,m^{-3}$)	37	0.2	0.3	36	0.0	0.1	39	0.2	0.2	41	0.3	0.4	153	0.2	0.2
Mg^{2+} ($\mu g\,m^{-3}$)	11	0.03	0.04	5	0.01	0.02	17	0.01	0.02	3	0.02	0.03	36	0.02	0.02
Ca^{2+} ($\mu g\,m^{-3}$)	10	0.04	0.1	7	0.1	0.1	6	0.1	0.1	0	–	–	23	0.1	0.1
SIA ($\mu g\,m^{-3}$)	37	7.3	10.2	36	4.5	4.6	40	8.7	10.6	41	10.8	11.9	154	7.1	9.5
SIA (%)	37	38	36	36	41	42	40	39	36	41	31	30	154	36	36
$\sum$WSII ($\mu g\,m^{-3}$)	37	8.0	11.2	36	4.6	4.9	40	9.9	11.4	41	11.9	13.0	154	8.0	10.2
$\sum$WSII (%)	37	42	41	36	43	44	40	43	41	41	34	33	154	41	40

Moreover, nitrate can easily react with sea-salt and crustal aerosols in coarse ($>2.5\,\mu m$) particles (Seinfeld & Pandis, 2006). This way, because ammonium is the main limiting ion for SIA generation (Erisman & Schaap, 2004), the estimation of SIA amounts was made after assessing the ionic balance between nitrate and sulfate versus ammonium. On annual basis, results of the linear regression between $NO_3^- + nssSO_4^{2-}$ and NH_4^+ (expressed as neq m^{-3}) show strong coefficients of determination, almost unitary slopes and very low intercept constants:

$$[NH_4^+] = 0.95[NO_3^- + nssSO_4^{2-}] + 1.5 \quad (R^2 = 0.96) \quad \text{for VL}$$

$$[NH_4^+] = 1.05[NO_3^- + nssSO_4^{2-}] - 8.6 \quad (R^2 = 0.97) \quad \text{for MC}$$

$$[NH_4^+] = 0.96[NO_3^- + nssSO_4^{2-}] - 6 \quad (R^2 = 0.98) \quad \text{for PS}$$

These results indicate that ammonium neutralizes almost completely sulfates and nitrates, allowing the estimation of SIA as the sum of NH_4^+, NO_3^- and $nssSO_4^{2-}$ masses.

On a yearly basis, SIA accounts for 9.5 μg m^{-3} (27% of $PM_{2.5}$ mass) in VL, 9.6 μg m^{-3} (28%) in MC and 9.5 μg m^{-3} (36%) in PS. Furthermore $PM_{2.5}$ concentrations strongly depend on SIA amounts ($r_{VL}=0.85$; $r_{MC}=0.73$; $r_{PS}=0.89$). These results indicate that similar values of SIA in term of masses are normally found in the whole area. As similar concentrations may indicate common origins and removal processes, these findings are a first evidence that SIA dynamics are more linked to regional processes than to local sources. Results are comparable with data collected in other sites of Po Valley, such as Milan, where SIA accounts for 43% of the $PM_{2.5}$ mass in the cold season and 37% in the warm season (Lonati et al., 2008).

The seasonal variation of nitrate inversely reflects the air temperature variations, with higher levels during the cold periods (Table 1). This is normally found in Western Europe (Schaap et al., 2004) and is favored by the combined effects of: (i) the larger availability of precursor NO_x due to the additional emission from domestic heating; (ii) the reaction between gaseous-phase NH_3 and HNO_3 to form particulate-phase NH_4NO_3 enhanced by the lower ambient temperatures and (iii) the volatilization of NO_3^- in warm periods. Sulfate presents higher concentrations in autumn and winter in all sites, but at PS its weight in the $PM_{2.5}$ mass is relatively higher.

4.3. Space variations

Inter-site differences of $PM_{2.5}$, NH_4^+, NO_3^- and SO_4^2 were evaluated on annual basis by one-way ANOVA. Major ions do not present significant statistical differences in the three sites, whereas $PM_{2.5}$ mass is significantly different at $\alpha=0.05$. Post-hoc tests show similar average values only between VL and MC. On annual basis, $PM_{2.5}$ appeared strongly correlated in the three sites ($r_{VL/MC}=0.90$; $r_{VL/PS}=0.92$; $r_{MC/PS}=0.88$), indicating that there are similar processes contributing to its formation, transport and removal processes in the area. However, correlation factors are different for data grouped seasonally. During autumn, winter and spring, correlations are generally higher ($r>0.84$) than in summer ($r_{VL/MC}=0.65$; $r_{VL/PS}=0.75$; $r_{MC/PS}=0.51$). This is probability due to different atmospheric circulation patterns, because sea/land breezes in summer enhance aerosol dispersion mainly in the coastal area.

4.4. Interpretation of results according to air mass dynamics

Recently, Masiol et al. (2010) detected a potential influence of regional-scale transport of fossil fuel related pollutants and SIA in Venice using back-trajectories analysis. Daily back trajectories were computed throughout the sampling period using MC as end point and then a cluster analysis was applied. After an analysis of the total spatial variance, the appropriate number of clusters was set to 7. The average back-trajectories associated to each cluster are reported in Fig. 2. Mean ± standard deviation of $PM_{2.5}$ and ions for each group are also summarized in Fig. 3.

Cluster 1 accounts for 4% of sampling period observations, includes trajectories from Northern Europe and exhibits very low concentrations of both $PM_{2.5}$ and WSII. Cluster 2 (19%) coming from Central part of Europe presents average concentrations similar to those of the full period. Cluster 3 (7%) indicates a Mediterranean provenance with low levels of both $PM_{2.5}$ and ions, except sodium. Cluster 4 is the most frequent (40%) and is characterized by air masses stagnating over the Po Valley. The average values are the highest for almost all variables, including $PM_{2.5}$ and SIA. Cluster 5 (5%) describes a westerly origin of trajectories with generally low concentrations of $PM_{2.5}$ and the majority of ions, but with relatively high values of Na^+ and Ca^{2+}. Cluster 6 (19%) and cluster 7 (6%) include the cases characterized by Northwesterly flows and generally concentrations are close to the average.

The classification of the air masses origins which arrive at Venice provide information on the potential impact of long-range transport of pollutants in Northeastern Italy. Results generally show that the levels of $PM_{2.5}$ increase when air masses move from Northern to Central and Northwestern Europe and drop when the trajectories originate from the Mediterranean region. However, the most worrying result is the relevant increase of $PM_{2.5}$ and SIA when the trajectories have spent most of their time in the Po Valley. This result confirms the strong influence of regional-scale transport on local air quality and at the same time opens a discussion about the possible success of local abatement strategies, such as traffic restrictions.

4.5. Role of local atmospheric circulation

Wind direction and speed are fundamental parameters to obtain a picture of the possible sources of emissions at a local scale. Wind speed is inversely proportional to pollutant concentration and would also produce a dilution effect on it, whereas its direction can help to extract information on source locations. In previous studies, particulate matter in Venice area has been studied in relation to micro-meteorological parameters, using short-term air pollution modeling (Rampazzo et al., 2008b), local circulation and back-trajectories (Masiol et al., 2010). These studies highlighted that air quality in the study area is closely associated with the local atmospheric circulation. In particular, the latter study detected that severe pollution events are often caused by local anthropogenic emissions, which accumulate in the atmosphere in the absence of significant advective transport.

In the present study, four main groups of samples with similar ionic composition were extracted on the basis of q-HCA for each station and containing generally the same samples, they were then interpreted similarly. Average values for each

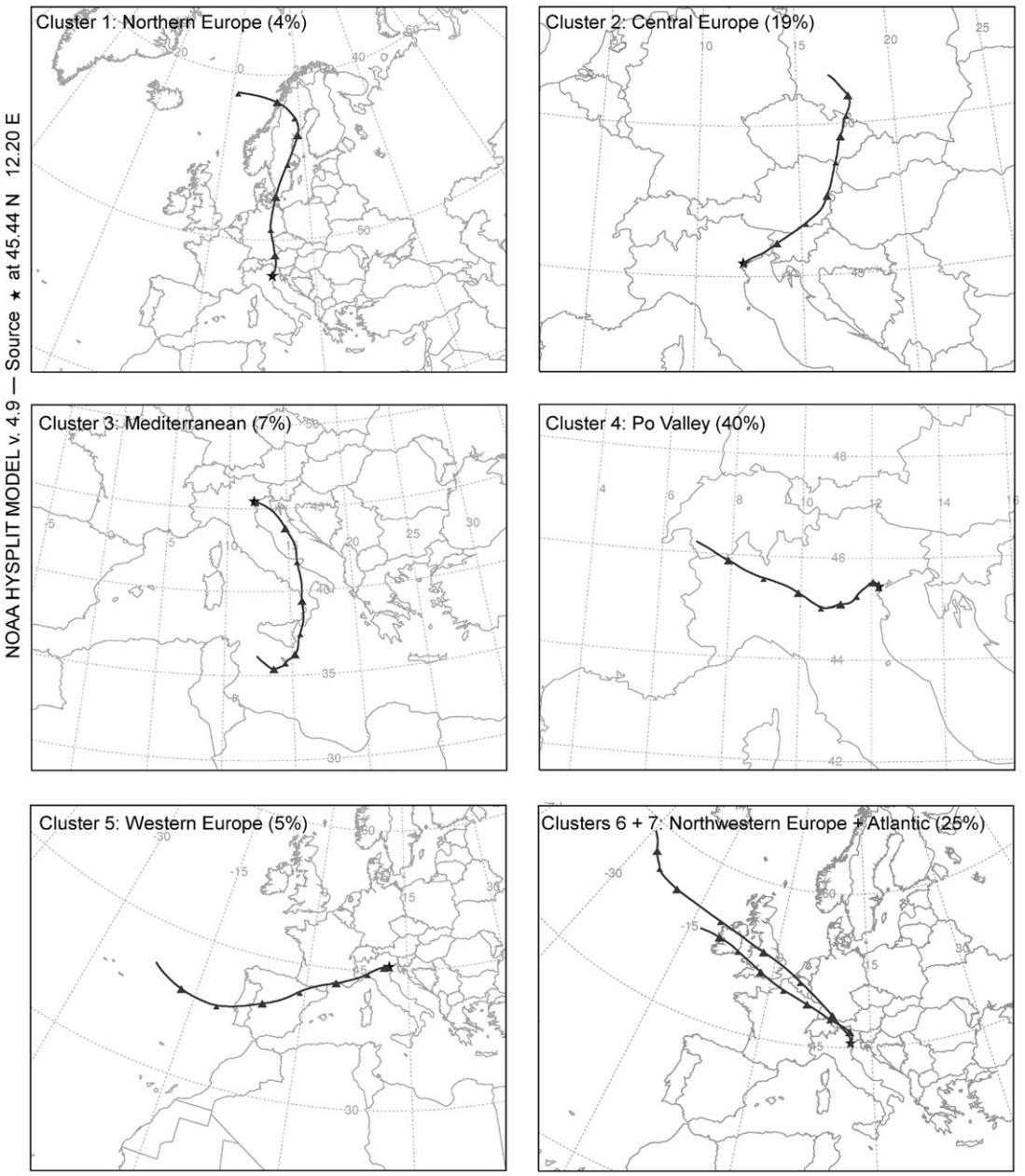

Fig. 2. Representative means of 4-days back-trajectory clusters.

group are summarized in Table 2. Wind roses for VL, that can be considered representative for all sites, are shown in Fig. 4. Individual wind roses must be interpreted by comparison with the full-period wind rose.

Group 1 shows lower concentrations of all variables and high values of sea-salt tracers (Na^+, Cl^-), except in VL where chlorine levels are very low. Prevailing winds come from quadrant I and II, with a relatively high average speed ($\sim$3.4 m s^{-1} MC, VL) and low percentages of calm ($\sim$1.5% MC, VL), whereas PS shows lower wind speed (1.9 m s^{-1}) and more frequent wind calm hours (8%). These results can be interpreted according to a previous study (Masiol et al., 2010), which indicated that the increase of the sea-salts component is due to local generation processes taking place along the coastline, mainly on Northeastern windy days. Moreover, high wind regimes enhance the atmospheric dispersion, with consequently low concentrations of $PM_{2.5,}$ sulfate, nitrate, ammonium and potassium.

Group 2 links days with higher concentrations of both $PM_{2.5}$ and ions, except sea-salt markers. The wind roses presents a lower average wind speed ($\sim$1.5 m s^{-1} MC and VL, 0.9 m s^{-1} PS) and more frequent wind calm ($\sim$8% MC and VL, 16% PS), but not a specific wind direction. During these days higher $PM_{2.5}$ levels and ion concentrations were found in both

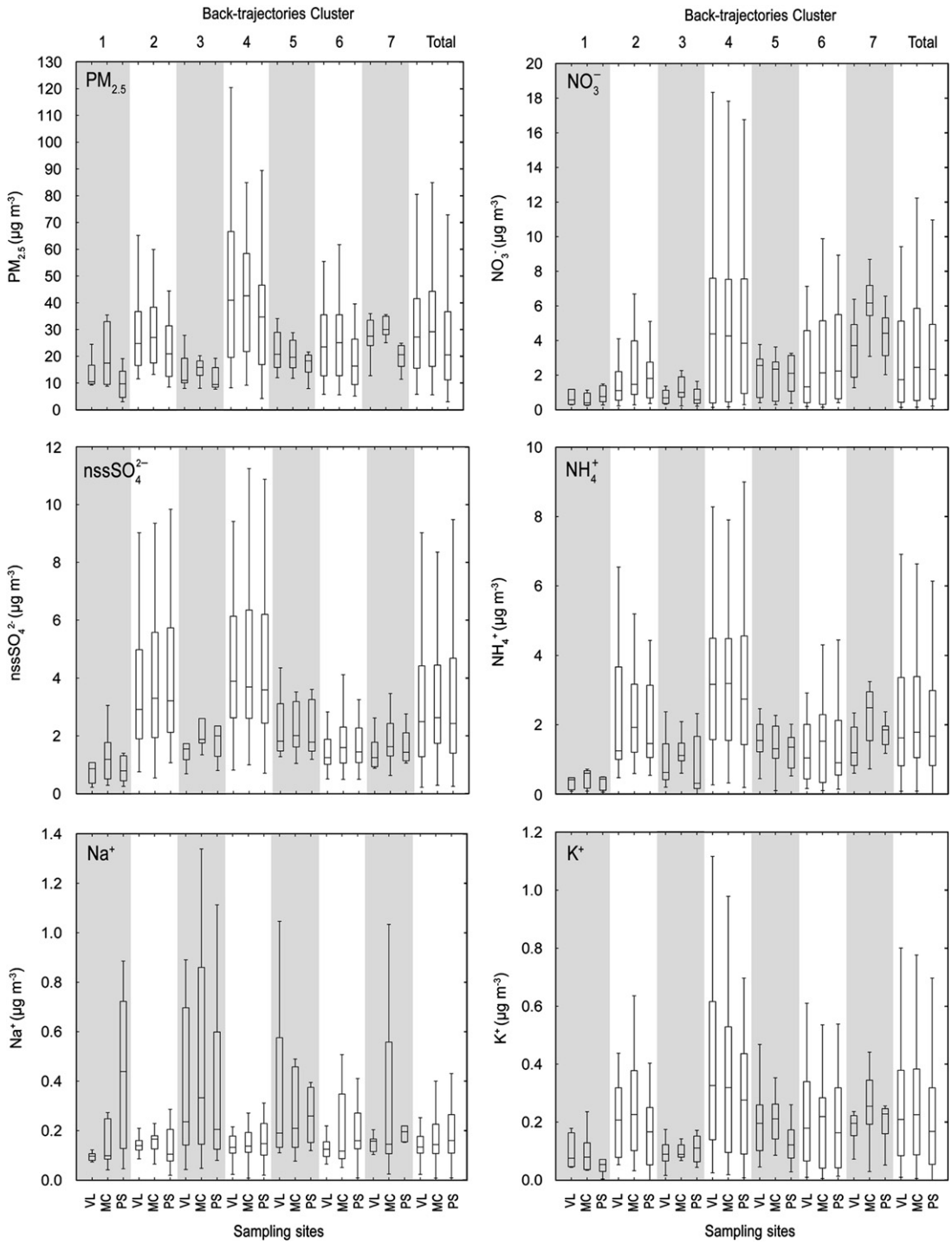

Fig. 3. Box-plots of $PM_{2.5}$ and most representative ions calculated for sampling included in each back-trajectories cluster, for each sampling site. Statistics are calculated including outliers, but outliers are not shown.

urban, industrial and coastal sites. These low-mobility atmospheric conditions tend to trap pollutants emitted locally by delaying their dispersion in the atmosphere.

Group 3 includes the largest number of samples (50%, 44% and 64% for VL, MC and PS, respectively), and generally presents average concentrations of all ions and $PM_{2.5}$ similar to the yearly ones. Wind roses show no significant differences with the full period rose. These samples could represent the general background pollution, the main common local $PM_{2.5}$ composition, when a common circulation pattern occurs.

Table 2
Average values for each group identified by *q*HCA analysis.

	Total (N)	**Spring** (N)	**Summer** (N)	**Autumn** (N)	**Winter** (N)	**$PM_{2.5}$** ($\mu g\ m^{-3}$)	**Cl^-** ($\mu g\ m^{-3}$)	**NO_3^-** ($\mu g\ m^{-3}$)	**SO_4^{2-}** ($\mu g\ m^{-3}$)	**$nssSO_4^{2-}$** ($\mu g\ m^{-3}$)	**Na^+** ($\mu g\ m^{-3}$)	**NH_4^+** ($\mu g\ m^{-3}$)	**K^+** ($\mu g\ m^{-3}$)	**SIA** ($\mu g\ m^{-3}$)	**%SIA**
Via Lissa (VL)															
Group 1 (sea-salt)	13	7	6	0	0	*14*	*0.06*	*0.8*	2.3	2.1	**0.88**	*0.8*	*0.08*	*3.6*	26
Group 2 (pollution)	15	6	0	3	6	**86**	**0.70**	**17.9**	**5.9**	**5.8**	0.16	**6.9**	**0.89**	**30.6**	**36**
Group 3 (general background)	**75**	22	23	19	11	21	0.08	1.9	*1.7*	*1.6*	*0.12*	1.1	0.17	4.6	*22*
Group 4 (cold period)	46	2	7	16	21	41	0.27	3.9	5.4	5.4	0.16	3.2	0.37	12.4	31
Malcontenta (MC)															
Group 1 (sea-salt)	14	14	0	0	0	25	**0.68**	4.4	2.6	2.4	**0.90**	2.0	0.22	8.7	35
Group 2 (pollution)	12	2	0	4	6	**71**	0.62	**13.3**	**5.3**	**5.2**	0.17	**5.9**	**0.75**	**24.4**	**36**
Group 3 (general background)	**64**	4	31	25	4	*18*	*0.06*	*0.9*	*2.4*	2.4	0.18	*1.0*	*0.11*	*4.3*	*24*
Group 4 (cold period)	54	10	0	13	31	48	0.42	6.3	4.6	4.6	*0.14*	3.7	0.47	14.6	31
Punta Sabbioni (PS)															
Group 1 (sea-salt)	20	3	0	15	2	18	0.35	2.3	*2.1*	*1.9*	**0.73**	*1.2*	*0.15*	*5.3*	*29*
Group 2 (pollution)	19	6	0	2	11	**64**	**0.56**	**13.7**	5.4	5.3	0.20	**5.6**	**0.56**	**24.6**	38
Group 3 (general background)	**98**	28	36	12	22	18	0.18	2.3	2.4	2.4	*0.15*	1.4	0.16	6.0	35
Group 4 (cold period)	17	0	0	11	6	38	*0.12*	3.9	**9.1**	**9.1**	0.21	4.2	0.27	17.2	**45**

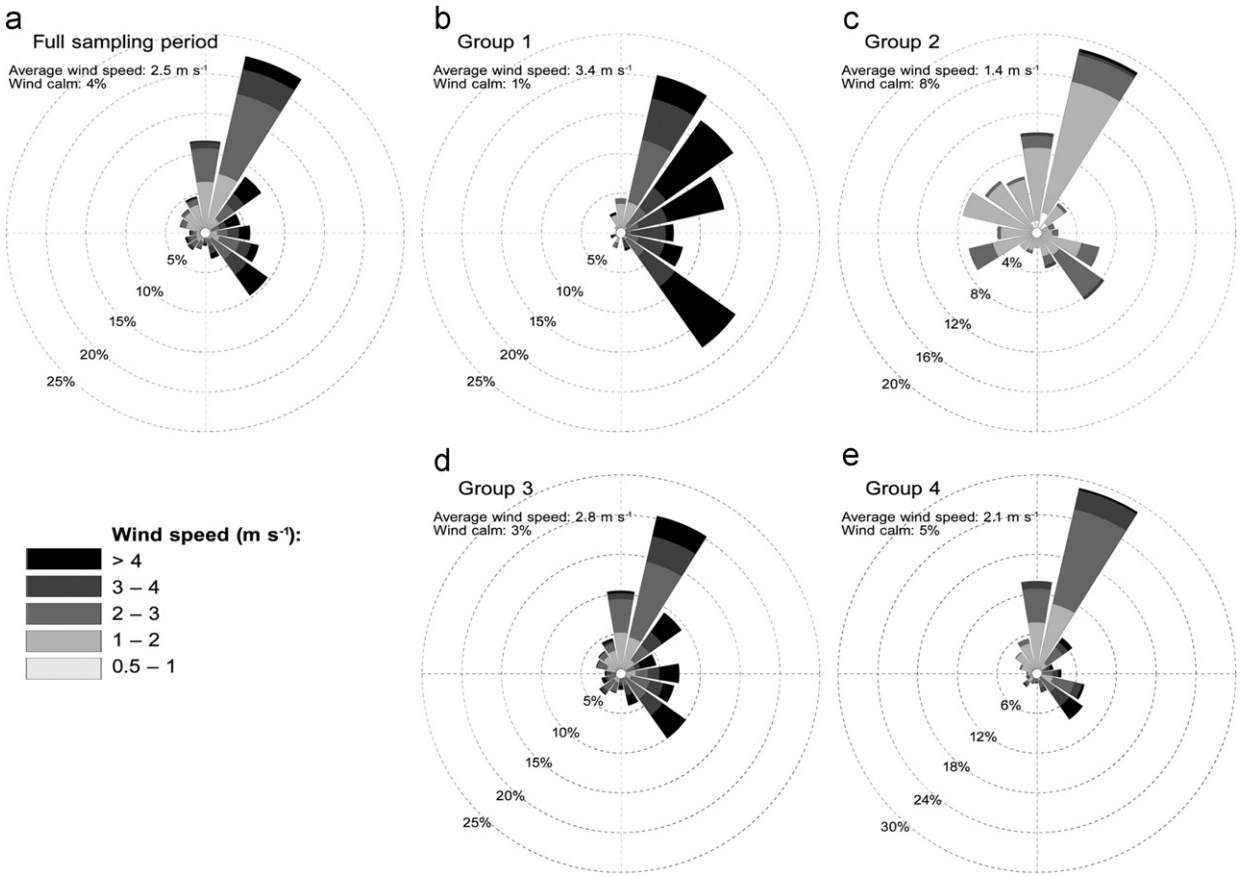

Fig. 4. Representative wind roses for VC site calculated in (a) the whole sampling period and (b, c, d, e) in each identified groups of samples by *q*HCA analysis.

Group 4 is mainly composed of samples with high SO_4^{2-} and $PM_{2.5}$ levels, lower wind speed and more wind calms compared to group 3. In addition, this group includes almost exclusively samples collected during the cold season. This group was interpreted as the typical cold period composition.

This approach reveals that air quality in this area is strongly influenced by the local atmospheric circulation. Common circulation patterns, group 3 (average annual) and 4 (typical of cold seasons), are associated with the general background pollution above which severe pollution episodes superimpose in particular atmospheric conditions.

4.6. Relationship between regional transport and local circulation

As previously noted, air quality in the area studied is strongly influenced by regional-scale transports. In particular high levels of $PM_{2.5}$ and SIA were observed when air masses were coming from the Po Valley. The role of local atmospheric circulation is also important.

To assess the relative importance of both regional and long-range transport and local circulation on air quality, air mass back trajectories were related to each cluster individuated by *q*HCA (Table 3).

Group 1-sea salt does not present a preferred air mass origin, because the increase of sea-salts components is due to local generation processes. Group 2-pollution and group 4-cold period are mainly associated with air masses coming from the Po Valley. Group 3-general background is composed of days characterized by Central Europe, Po Valley and NW Europe back trajectories. This group, representing the main common local $PM_{2.5}$ composition, is associated to the most frequent back-trajectories over the sampling period. On the basis of SIA concentrations, events with high pollution loads were identified that exceeded the annual average. These days are related to group 2-pollution and group 4-cold period in VL and MC and also to group 3 in PS. Back-trajectories coming from Po Valley represented 73%, 60% and 68% of total events in VL, MC and PS, respectively.

Groups 2 and 4 are characterized by low average wind speed ($1.4\,m\,s^{-1}$ and $2.1\,m\,s^{-1}$) and high wind calm percentages (8% and 5%). In these low-mobility atmospheric conditions, pollutants coming from the Po Valley add up to a general background pollution, resulting in heavy pollution events with high PM and SIA levels.

Table 3
Air mass back-trajectories clusters related to each groups individuated by *q*HCA.

	Total N	Group 1 (%) Northern Europe	Group 2 (%) Central Europe	Group 3 (%) Mediterranean	Group 4 (%) Po Valley	Group 5 (%) Western Europe	Group 6 (%) NW Europe	Group 7 (%) North Atlantic
Via Lissa (VL)								
All samples	149	4	19	7	**42**	3	20	5
Group 1 (sea-salt)	13	8	15	15	23	8	31	0
Group 2 (pollution)	15	0	7	0	**87**	0	7	0
Group 3 (general background)	75	7	23	8	20	3	29	11
Group 4 (cold period)	46	0	20	4	**67**	2	7	0
Heavy SIA Events	48	0	17	2	**73**	0	6	2
Malcontenta (MC)								
All samples	144	6	20	6	**39**	1	22	6
Group 1 (sea-salt)	14	7	21	21	0	0	43	7
Group 2 (pollution)	12	0	8	0	**83**	0	0	8
Group 3 (general background)	64	6	23	6	27	3	27	8
Group 4 (cold period)	54	6	19	4	**54**	0	15	4
Heavy SIA Events	58	2	19	0	**60**	0	10	9
Punta Sabbioni (PS)								
All samples	154	5	19	6	**41**	3	20	6
Group 1 (sea-salt)	20	20	15	15	20	0	20	10
Group 2 (pollution)	19	0	10	0	**68**	0	16	5
Group 3 (general background)	98	4	19	7	36	4	23	6
Group 4 (cold period)	17	0	29	0	**65**	0	6	0
Heavy SIA Events	56	0	16	0	**68**	0	13	4

Table 4
Mean of local contribution of $PM_{2.5}$, NO_3^-, $nssSO_4^{2-}$ and NH_4^+ express in $\mu g\,m^{-3}$ and as percentage on mass.

	$PM_{2.5\,local}$		$NO_{3\,local}^-$		$nssSO_{4\,local}^{2-}$		$NH_{4\,local}^+$	
	$\mu g\,m^{-3}$	%	$\mu g\,m^{-3}$	%	$\mu g\,m^{-3}$	%	$\mu g\,m^{-3}$	%
Via Lissa (VL)								
All samples	9.8	27.7	1.6	23.8	0.5	11.6	0.6	24.3
Spring	11.3	26.3	2.9	23.1	1.0	20.7	0.8	24.2
Summer	4.5	31.2	0.1	18.3	0.4	11.3	0.1	13.8
Autumn	5.7	24.5	1.6	32.6	0.2	10.1	0.3	20.2
Winter	15.5	28.6	1.4	23.0	0.4	9.3	0.8	30.4
Heavy SIA Events	16.4	25.7	2.4	24.8	0.7	13.4	1.0	20.0
Malcontenta (MC)								
All samples	9.8	29.9	1.4	27.8	0.7	18.5	0.6	29.3
Spring	10.4	31.7	1.9	35.6	0.5	17.4	0.8	39.0
Summer	8.9	40.5	0.9	37.3	1.3	20.3	0.1	18.6
Autumn	6.6	25.4	0.7	24.3	0.5	18.6	0.3	23.0
Winter	12.5	24.8	1.3	21.9	0.6	17.7	0.8	30.6
Heavy SIA Events	12.6	23.8	1.8	28.4	1.2	17.3	0.9	24.1

These results indicate that SIA levels, and consequently $PM_{2.5}$ concentrations, depend on regional scale transport processes and also are linked to local atmospheric circulation.

On the basis of this observation, the Lenschow approach was applied to estimate local contribution on PM and SIA components in VL and MC. Yearly, local sources contribute for 9.8 $\mu g\,m^{-3}$ of $PM_{2.5}$ amounting to 28% and 30% of masses in VL and MC, respectively. Seasonally, the highest local contributions were observed in spring and winter in particular for $PM_{2.5}$, NO_3^- and NH_4^+. In summer, the local contribution is lower than in other seasons but accounts for the highest percentages in $PM_{2.5}$ masses (Table 4). Local $nssSO_4^{2-}$ contribution is lower compared to other ions and shows similar average concentrations and percentage over different periods and heavy SIA events. On this basis, $nssSO_4^{2-}$ levels are mainly related to regional transport processes.

During heavy SIA events, such as those mainly occurring when air masses come from Po Valley, local contribution on PM increases. Average values are 16.4 $\mu g\,m^{-3}$ (26%) and 12.6 $\mu g\,m^{-3}$ (24%) in VL and MC, respectively. Nevertheless, considering the mass percentage, no significant variations have been observed for all periods and samples. In days with low wind speed ($\sim$1.9 $m\,s^{-1}$) and high percentage of wind calm ($\sim$5%) pollutants coming from Po Valley are retained. In conclusion, heavy SIA events are mainly due to a regional contribution and are enhanced by scarce atmospheric dispersion that tend to trap pollutants.

5. Conclusions

In this work a simple and effective approach is proposed to discriminate the role of regional and long-range transport episodes and local sources on $PM_{2.5}$ formation and its ionic composition. This method combines $PM_{2.5}$ chemical compositions with back-trajectories statistical analysis and local atmospheric circulation (wind speed and direction).

To evaluate the influence of regional and long-range transports, daily back trajectories were calculated and samples were statistically sorted into groups. Then, a cluster analysis on chemical data was performed to gather samples with similar compositions and the influence of local atmospheric circulation was studied by analyzing wind data related to each group. Finally, clusters from back-trajectories were matched with groups resulting from *q*HCA and local contribution for $PM_{2.5}$ and major ions was estimated using the Lenschow approach.

The levels of $PM_{2.5}$ increase when the trajectories move from Northern, Central and Northwestern Europe and drop when air masses originate in the Mediterranean region. High levels of $PM_{2.5}$ and major ions were observed when the trajectories had spent most of their time in the Po Valley. Results reveal an influence of local atmospheric circulation on high pollution events associated with low wind speed and high wind calm but not with a specific wind direction. In other words, high wind regimes enhance the atmospheric dispersion, and consequently lower the concentrations of $PM_{2.5}$, sulfate, nitrate, ammonium and potassium.

In particular, heavy SIA events occur in correspondence of days characterized by stable atmospheric conditions and air masses coming from the Po Valley. In these circumstances, a regional pollution is added to a general contaminated background, resulting in high $PM_{2.5}$ and SIA levels.

On an annual basis, local sources contribute for 27.7% and 29.9% of $PM_{2.5}$ in VL and MC, respectively. Seasonally, the highest local contributions were observed in spring and winter in particular for $PM_{2.5}$, NO_3^- and NH_4^+, whereas the local shares of $nssSO_4^{2-}$ are similar in different periods. During intense SIA events the local contribution to PM increases, but considering the mass percentage, no significant variations have been observed over all periods and samples. Hence, heavy SIA events are mainly due to a regional contribution and are related to scarce atmospheric dispersion that tend to trap pollutants.

This study demonstrates that pollutants concentrations in the studied area mainly depend on both regional transport processes and local atmospheric circulation. Results represent a significant contribution to the knowledge of $PM_{2.5}$ chemistry and dynamics in Northeastern Italy. Moreover, the relevant role of the secondary component on $PM_{2.5}$ mass coming from Po Valley suggests that abatement measures must include not only local actions (e.g. traffic restrictions), but also coordinated regional-scale control strategies.

The proposed approach can be a useful tool to better understand the aerosol sources, its dynamics and generation processes and it is easily applicable to other atmospheric environments.

Acknowledgment

This study presents a part of the results obtained in the framework of the project "Study of secondary particulate matter in the Venice area", financially supported by Ente Zona Industriale di Porto Marghera (http://www.entezona.it/). The authors are grateful to ARPAV managers and technicians, in particular Dr. Gianmaria Formenton and Dr. Enzo Tarabotti, for their valuable support, to Prof. Francesco Pinna, Dr. Michela Signoretto and Dr. Elena Ghedini for their analytical support and the Comando Zona Fari e Segnalamenti Marittimi di Venezia for logistics. The authors gratefully acknowledge having used the HYSPLIT transport and dispersion model compiled by the NOAA Air Resources Laboratory (ARL) and available in the READY website (http://www.arl.noaa.gov/ready.php).

References

ARIANET (2005). SURFPRO, SURface-atmosphere interFace PROcessor, Version 2.2, User's Guide. Arianet R2005.11, Milano, April.

Aria Technologies (2001). MINERVE Wind Field Models Version 7.0, General Design Manual ARIA Report. Aria Technologies, Paris.

ARPAV (Environmental Protection Agency of Veneto Region) (2010a). The Quality of the Air in the Municipality of Venice. Annual Report 2009, p. 113 [in Italian].

ARPAV (Environmental Protection Agency of Veneto Region) (2010b). Regional relation of air quality, pp. 59 [in Italian]. Available from: 〈http://www.arpa.veneto.it/Download/Relazione_regionale_aria_2009.pdf〉.

CEN (Comité Européen de Normalisation) (2005). Ambient Air Quality—Standard Gravimetric Measurement Method for the Determination of the $PM_{2.5}$ Mass Fraction of Suspended Particulate Matter. Ref. No. EN14907:2005:E.

Centanni, E., Pecorari, E., Squizzato, S., Sartoretto, F., Pavoni, B., Rampazzo, G., Rampado, E., & Buttini, P. (2009). Analyses on $PM_{2.5}$ in the Venice area: a first approach to secondary aerosol characterization. In: Proceedings of 18th International Conference on Nucleation and Atmospheric Aerosols. Smolik, J., O'Dowd C., (Eds.), 10–14 August, Prague, Czech Republic, pp. 870–873.

Draxler, R.R., & Rolph, G.D. (2011). HYSPLIT (HYbrid Single-Particle Lagrangian Integrated Trajectory) Model access via NOAA ARL READY. Website 〈http://ready.arl.noaa.gov/HYSPLIT.php〉. NOAA Air Resources Laboratory, Silver Spring, MD.

Draxler, R., Stunder, B., Rolph, G., Stein, A., & Taylor, A. (2009). HYSPLIT4 User's Guide, Version 4.9. Available from: 〈http://www.arl.noaa.gov/documents/reports/hysplit_user_guide.pdf〉 (last access: February 1, 2011).

EC (European Commission) (2004). CAFE Working Group on Particulate Matter (Ed.), Second Position Paper on Particulate Matter, p. 234.

EC (European Commission) (2008). Council Directive 2008/50/EC of the European Parliament and of the Council of 21 May 2008 on ambient air quality and cleaner air for Europe. Official Journal of European Communications. L152/1, 11/6/2008.

EEA (European Environment Agency) (2005). The European Environment—State and Outlook 2005. Copenhagen, Denmark.

EEA, European Environment Agency (2010). AirBase—The European Air Quality Database. Available from: 〈http://www.eea.europa.eu/themes/air/airbase〉 (last access: December 23, 2010).

Erisman, J.W., & Schaap, M. (2004). The need for ammonia abatement with respect to secondary PM reductions in Europe. *Environmental Pollution*, *129*, 159–163.

Glavas, S.D., Nikolaki, P., Ambatzoglou, D., & Mihalopoulos, N. (2008). Factors affecting the seasonal variation of mass and ionic composition of $PM_{2.5}$ at a central Mediterranean coastal site. *Atmospheric Environment*, *42*, 5365–5373.

Hamed, A., Joutsensaari, J., Mikkonen, S., Sogacheva, L., Dal Maso, M., Kulmala, M., Cavalli, F., Facchini, M.C., Decesari, S., Mircea, M., Lehtinen, K.E.J., & Laaksonen, A. (2007). Nucleation and growth of new particles in Po-Valley, Italy. *Atmospheric Chemistry and Physics*, *7*, 335–376.

Hazenkamp-von Arx, M.E., Götschi, T., Ackermann-Liebrich, U., Bono, R., Burney, P., Cyrys, J., Jarvis, D., Lillienberg, L., Luczynska, C., Maldonado, J.A., Jaén, A., de Marco, R., Mi, Y., Modig, L., Bayer-Oglesby, L., Payo, F., Soon, A., Sunyer, J., Villani, S., Weyler, J., & Künzli, N. (2004). $PM_{2.5}$ and NO_2 assessment in 21 European study centres of ECRHS II: annual means and seasonal differences. *Atmospheric Environment*, *38*, 1943–1953.

Lenschow, P., Abraham, H.-J., Kutzner, K., Lutz, M., Preuß, J.-D., & Reichenbächer, W. (2001). Some ideas about the sources of PM_{10}. *Atmospheric Environment*, *35*, S23–S33.

Lonati, G., Giugliano, M., & Ozgen, S. (2008). Primary and secondary components of $PM_{2.5}$ in Milan (Italy). *Environment International*, *34*, 665–670.

Masiol, M., Rampazzo, G., Ceccato, D., Squizzato, S., & Pavoni, B. (2010). Characterization of PM_{10} sources in a coastal area near Venice (Italy): an application of factor-cluster analysis. *Chemosphere*, *80*, 771–778.

Polichetti, G., Cocco, S., Spinali, A., Trimarco, V., & Nunziata, A. (2009). Effects of particulate matter (PM_{10}, $PM_{2.5}$ and PM_1) on the cardiovascular system. *Toxicology*, *261*, 1–8.

Pope, C.A., & Dockery, D.W. (2006). Health effects of fine particulate air pollution: lines that connect. *Journal of the Air and Waste Management Association*, *56*, 709–742.

Prodi, F., Belosi, F., Contini, D., Santachiara, G., Di Matteo, L., Gambaro, A., Donateo, A., & Cesari, D. (2009). Aerosol fine fraction in the Venice Lagoon: particle composition and sources. *Atmospheric Research*, *92*, 141–150.

Putaud, J.P., Raes, F., Van Digenen, R., Brüggemann, E., Facchini, M.-C., Decesari, S., Fuzzi, S., Gehrig, R., Hüglin, C., Laj, P., Lorbeer, G., Maenhaut, W., Mihalopoulos, N., Müller, K., Querol, X., Rogriguez, S., Schneider, J., Spindler, G., ten Brink, H., Tørseth, K., & Wiedensohler, A. (2004). A European aerosol phenomenology—2: chemical characteristics of particulate matter at kerbside, urban, rural and background sites in Europe. *Atmospheric Environment*, *38*, 2579–2595.

Putaud, J.-P., Van_Dingenen, R., Alastuey, A., Bauer, H., Birmili, W., Cyrys, J., Flentje, H., Fuzzi, S., Gehrig, R., Hansson, H.C., Harrison, R.M., Herrmann, H., Hitzenberger, R., Hüglin, C., Jones, A.M., Kasper-Giebl, A., Kiss, G., Kousa, A., Kuhlbusch, T.A.J., Löschau, G., Maenhaut, W., Molnar, A., Moreno, T., Pekkanen, J., Perrino, C., Pitz, M., Puxbaum, H., Querol, X., Rodriguez, S., Salma, I., Schwarz, J., Smolik, J., Schneider, J., Spindler, G., ten_Brink, H., Tursic, J., Viana, M., Wiedensohler, A., & Raes, F. (2010). A European aerosol phenomenology—3: physical and chemical characteristics of particulate matter from 60 rural, urban, and kerbside sites across Europe. *Atmospheric Environment*, *44*, 1308–1320.

Rampazzo, G., Masiol, M., Visin, F., & Pavoni, B. (2008a). Gaseous and PM_{10}-bound pollutants monitored in three environmental conditions in the Venice area (Italy). *Water, Air, Soil and Pollution*, *195*, 161–176.

Rampazzo, G., Masiol, M., Visin, F., Rampado, E., & Pavoni, B. (2008b). Geochemical characterization of PM10 emitted by glass factories in Murano, Venice (Italy). *Chemosphere*, *71*, 2068–2075.

Rolph, G.D. (2011). Real-time Environmental Applications and Display sYstem (READY). Website 〈http://ready.arl.noaa.gov〉. NOAA Air Resources Laboratory, Silver Spring, MD.

Rossini, P., Matteucci, G., & Guerzoni, S. (2010). Atmospheric fall-out of metals around the Murano glass-making district (Venice, Italy). *Environmental Science and Pollution Research*, *17*, 40–48.

Salvador, P., Artíñano, B., Querol, X., & Alastuey, A. (2008). A combined analysis of backward trajectories and aerosol chemistry to characterise long-range transport episodes of particulate matter: the Madrid air basin, a case study. *Science of Total Environment*, *390*, 495–506.

Seinfeld, J.H., & Pandis, S.N. (2006). *Atmospheric Chemistry and Physics. From Air Pollution to Climate Change* (2nd ed.). John Wiley & Sons: New York.

Schaap, M., van Loon, M., ten Brink, H.M., Dentener, F.J., & Builtjes, P.J.H. (2004). Secondary inorganic aerosol simulations for Europe with special attention to nitrate. *Atmospheric Chemistry and Physics*, *4*, 857–874.

Sogacheva, L., Hamed, A., Facchini, M.-C., Kulmala, M., & Laaksonen, A. (2007). Relation of air mass history to nucleation events in Po Valley, Italy, using back trajectories analysis. *Atmospheric Chemistry and Physics*, *7*, 839–853.

Stohl, A. (1998). Computation, accuracy and applications of trajectories—a review and bibliography. *Atmospheric Environment*, *32*, 947–966.

Stortini, A.M., Freda, A., Cesari, D., Cairns, W.R.L., Contini, D., Barbante, C., Prodi, F., Cescon, P., & Gambaro, A. (2009). An evaluation of the $PM_{2.5}$ trace elemental composition in the Venice Lagoon area and an analysis of the possible sources. *Atmospheric Environment*, *43*, 6296–6304.

Valkama, I. & Kukkonen, J. (Eds.) (2004). Identification and Classification of Air Pollution Episodes in terms of Pollutants, Concentration Levels and Meteorological Conditions. Deliverable 2.1 of the FUMAPEX Project, Helsinki, 30pp.